JOURNAL OF MATERIALS SCIENCE 20 (1985) 2807–2822

Effect of thermal treatments on the fracture behaviour of notched polyethylene terephthalate ribbons

KLAUS FRIEDRICH
Polymer and Composites Group, Technical University Hamburg-Harburg, 2100 Hamburg 90, West Germany
STOYKO FAKIROV
Faculty of Chemistry, Sofia University, 1126 Sofia, Bulgaria

The application of different thermal treatment procedures to thin polyethylene terephthalate (PET) sheets yields to microstructures of different molecular weight/degree of crystallinity combination. As a consequence, variations in the mechanical properties, especially the fracture properties and the particular fracture mechanisms occur. This is demonstrated in this paper by measurements of elastic modulus, maximum stress, failure initiation energy, and total work to fracture of notched PET-ribbons. Failure mechanisms analysed by the use of optical and scanning electron microscopy vary between highly ductile via semi-brittle after crazing, to absolute brittle at very low stresses. The results are summarized in terms of a three-dimensional failure energy map divided into regions of particular failure behaviour for particular molecular weight/degree of crystallinity combination. In addition, the typical values of material strength, defined as the product of resistance to damage initiation (maximum stress) and crack propagation (total work to failure) are given for each region. The optimum fracture resistance was achieved for PET material with moderately low molecular weight and moderately high degree of crystallinity.

1. Introduction

Many studies of the recent years have shown that the mechanical behaviour of thermoplastic polymers is highly influenced by molecular and morphological parameters of the materials investigated [1–4]. In particular, it was shown that the molecular weight of a polymeric material is of special importance if fracture properties are considered. An increase in molecular weight usually leads to enhancements of material properties such as impact resistance, elongation to break and fracture toughness [5, 6]. Recent studies on the fatigue crack propagation in different thermoplastics have also shown that the crack growth resistance is improved the higher is the molecular weight [7, 8]. As known from other studies, similar effects can be obtained if the material has a semi-crystalline microstructure. Normally a high degree of crystallinity yields property improvements in both, strength and modulus of the material [9, 10]. Also, toughness and resistance to fatigue crack propagation are usually influenced by the existence of crystals in a positive manner [11, 12]. It has to be mentioned, however, that when talking about effects of a crystalline microstructure the degree of crystallinity is not the only parameter which characterizes the influence of this kind of microstructure. On the contrary, often it is the arrangement of the crystalline arrays and the surrounding amorphous regions, i.e. the morphology of the semi-crystalline thermoplastic, which determines much more effectively the mechanical properties and the failure mechanisms. Usually, for a given degree of crystallinity, a material with

0022–2461/85 $03.00 + .12

a fine spherulitic structure proves to be much better than the arrangements of crystalline regions in the form of very coarse spherulites [13–16].

The interacting influence of the property profile of thermoplastic polymers due to variations in both molecular weight and parameters of the semi-crystalline microstructure, has been demonstrated in some recent publications [17, 18]. It can be stated in general, that the molecular weight as well as the degree of crystallinity must be optimized, not maximized in order to receive the best results with respect to a good property profile. Where these optimum conditions are located is a function of the molecular structure of the particular polymer investigated and the special properties required. As a further contribution for clarifying this subject, in this paper it is outlined how modulus, strength, fracture energy, and the resulting failure mechanisms of notched polyethylene terephthalate (PET) ribbons vary if the material is subjected to various thermal histories. By the latter procedures variations in the molecular weight as well as the degree and perfections of crystallinity can be obtained.

2. Experimental details

2.1. Material, thermal treatments and structural characterization

Commercial sheets of polyethylene terephthalate (PET) having a thickness of 0.4 mm were used as starting material (provided through the courtesy of E. I. Du Pont de Nemours Inc, Wilmington, Delaware, USA). Following storage in a dry-box, the material sheets were subjected to different thermal treatment procedures in order to obtain variations in both molecular weight and degree of crystallinity:

Procedure A: commercial samples were annealed at constant temperatures (100, 200, 260° C) for 6 h in a dry nitrogen atmosphere. After subsequent quenching in ice-water specimens were cut and returned to the dry-box until testing.

Procedure A + A: a two-step annealing process was carried out with the starting material in a way that first the polymer was treated in dry nitrogen atmosphere at 260° C and then after quenching in ice-water a second annealing process followed at 250° C in air.

Procedure P: from the starting material, samples with higher molecular weight were prepared by using the well known technique of additional solid state post-condensation [19, 20]. Sheets were held at 250° C for 60 h in a vacuum atmosphere (3 to 5 Torr). In this way, an increase in molecular weight as well as a high degree of crystallinity was generated in the samples. In order to eliminate, or at least to reduce strongly, the degree of crystallinity, the same samples sealed in aluminium foil were moulded rapidly by holding them for 1 to 2 minutes between metal blocks having a temperature of 270 ± 3° C. After subsequent quenching in ice-water, fully transparent sheets were obtained.

Procedure P + A: after having experienced procedure P, several sheets were annealed at different temperatures (100, 200, 250, 260° C) in a nitrogen atmosphere for 6 h [21].

Values of the molecular weight were determined viscosimetrically after the different thermal treatments. The intrinsic viscosity, $[\eta]$, was calculated from the specific viscosity, η_{Sp}, by the equation

$$[\eta] = \frac{(1 + 1.4\,\eta_{Sp})^{1/2} - 1}{0.35} \qquad (1)$$

on the basis of measurements performed at 20° C in the solvent phenol–tetrachlorethan (1:1). Using these values, the molecular weight, $\bar{M}_v$, could be calculated by the well known relationship

$$[\eta] = K\bar{M}_v^{\alpha} \qquad (2)$$

in which the parameters K and α have the values 1.27×10^{-4} and 0.86, respectively [22]. Additional control measurements of the number average molecular weight, $\bar{M}_n$, had been carried out with samples of procedures A and P + A after annealing at 200° C, using a gel permeation chromatography (GPC) apparatus.

The degree of crystallinity was checked in two different ways: by generating differential scanning calorimetric thermograms (DSC) and by using a density gradient column. By the DSC method a determination of the degree of crystallinity, w_c (DSC), is derived from measurements of the heat of fusion, ΔH_{exp}, according to:

$$w_c(\mathrm{DSC}) = \frac{\Delta H_{exp}}{\Delta H_m^{\circ}} \qquad (3)$$

where ΔH_m° is the heat of fusion (per mol of repeated unit) of an ideal PET crystal. For ΔH_m° we adopted the value of 5.8 kcal mol^{-1} = 24.3 kJ mol^{-1}, given by Wunderlich [23] which is very close to those values proposed by other authors [24]. All the DSC measurements were carried out using a Du Pont differential thermal analyser, model 999, in an air atmosphere (specimen weight

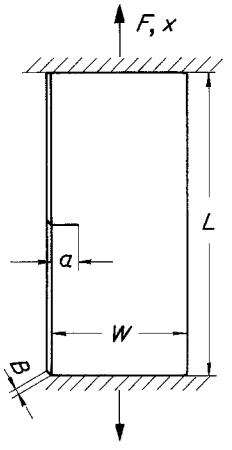

Figure 1 Geometry of single edge notched specimen configuration: crack length $a = 2$ mm, thickness $B = 0.4$ mm, free specimen length $L = 22$ mm, width $W = 10$ mm, notch cross-section $A_N = B(W\text{-}a) = 3.2$ mm^2; F = load (N), x = displacement (mm).

equal to 5 mg). The heating rate was 20° C min^{-1}. The densities of all the different samples were measured by means of a gradient column using a mixture of carbon tetrachloride and hexan. The crystallinity index, w_c (ρ), was calculated from

$$w_c(\rho) = \frac{\bar{\rho} - \rho_a}{\rho_c - \rho_a} \quad (4)$$

where $\rho_a = 1.335$ g cm^{-3} and $\rho_c = 1.515$ g cm^{-3} are the densities of the fully amorphous and of the completely crystalline polymer, respectively [25–27]. $\bar{\rho}$ is the experimentally determined density of the material investigated.

Further characterization of the morphological structure of the different polymer samples was performed with transmitting polarized light in an optical microscope.

2.2. Mechanical testing

Fig. 1 illustrates the geometry of single edge notched specimens cut from the thermally treated sheets and used for the fracture experiments. The latter were conducted on a static testing machine under stroke control in a laboratory environment (23° C and an average relative humidity of 30%) at a cross-head speed of 5 mm min^{-1}. From the load F–displacement x curves the following material properties were determined:

(a) elastic modulus, E, (under the influence of reduced cross section due to the notch);

(b) the notch strength, σ_{max}, as calculated from the maximum load divided by the notch cross-section, A_N;

(c) the energy for damage initiation, W_{max}, defined as the area under the load–displacement curve up to the load maximum (dimension Nm) divided by the notch cross-section, A_N;

(d) the total fracture energy, W_{tot}, which is proportional to the whole area under the load–displacement curve (equivalent to the work for complete specimen separation).

2.3. Analysis of failure mechanisms

Deformation modes and fracture surfaces were examined using an optical microscope (reflected and transmitted light) and a scanning electron microscope (SEM), respectively. Prior to the SEM studies, coating of the fracture surfaces with a thin gold layer was necessary.

3. Results and discussion

3.1. Microstructural characterization

As shown in Table I, the different procedures of thermal treatment have generated a variety of

TABLE I Relationship of thermal treatment procedure and degree of crystallinity as well as molecular weight in the materials PET-1 to PET-10

Specimen number	Procedure of thermal treatment	Annealing temperature T_a(° C)	Annealing time t_a(h)	Degree of crystallinity $w_c(\rho)$	Degree of crystallinity w_c(DSC)	$\bar{w}_c$ (%)	Molecular weight $\bar{M}_v$
PET-1	Commercial	–	–	56	35	45	21 100
PET-2	A	100	6	56	37	46	22 400
PET-3	A	200	6	57	48	52	21 000
PET-4	A	260	6	58	52	55	41 600
PET-5	A + A	260(N_2) 250 (air)	6 6	59	54	56	17 400
PET-6	P	–	–	3	9	6	32 400
PET-7	P + A	100	6	4	6	5	31 300
PET-8	P + A	200	6	20	28	24	33 200
PET-9	P + A	250	6	58	54	56	41 100
PET-10	P + A	260	6	57	55	56	58 000

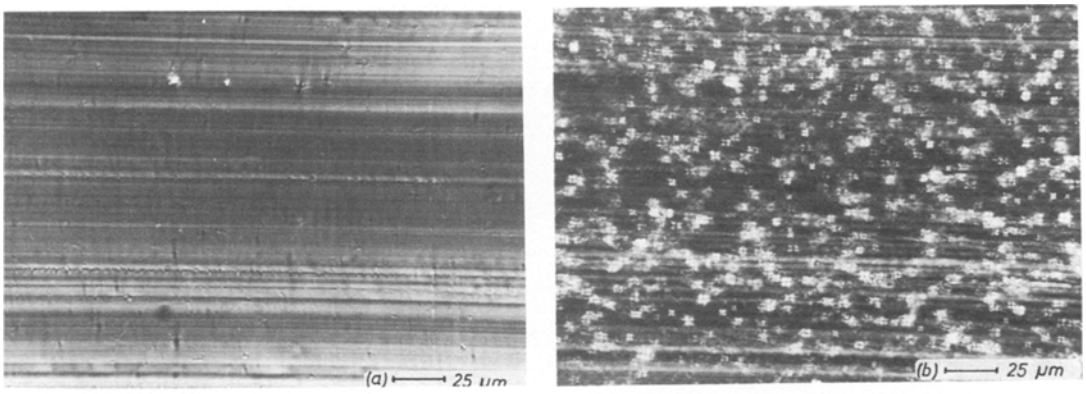

Figure 2 Transmitted light optical micrographs of the morphologies in specimens PET-6 to 8 (a) and PET-1 to 5, 9, 10 (b). The bright lines on both photos are due to the microtome cutting procedure of the thin sections for transmission.

different crystallinity–molecular weight combinations. Considering the arithmetic average of two crystallinity measurements as a relevant value of the degree of crystallinity in each specimen, the starting material had already a moderately high percentage of crystals ($\bar{w}_c = 45\%$). On the other hand, the molecular weight, $\bar{M}_v$, was rather low. The annealing procedure A at temperatures of 100 and 200° C caused a clear increase in the degree of crystallinity which was mainly detectable by the DSC method, whereas no significant variation in the molecular weight had occurred. This changed drastically when annealing was performed at a temperature of 260° C. Under these circumstances, a polycondensation in the solid state had yielded a two-fold higher molecular weight, simultaneously the degree of crystallinity was further increased. As known from other investigations, especially at temperatures above 150° C, one has to expect an additional extent of secondary crystallization leading to further crystalline perfection as well as increasing thickness of the crystalline lamellae. A second step of annealing in air of 250° C provides a further enhancement of the degree of crystallinity, but at the same time a significant molecular degradation, probably due to oxidation effects, takes place.

Specimen PET-6 represents the microstructural condition after the thermal treatment P by which a 1.5-fold higher molecular weight (as compared to the commercial product) and a very low degree of crystallinity was obtained. Further annealing at temperatures below 250° C gave again a stepwise increase in the degree of crystallinity. Additional changes in the molecular weight were only obtained when the annealing temperature was in the range 250° C or above (specimen PET-9 and 10). Control measurements of the weight and number average molecular weights of specimens PET-3 and PET-8 as derived by the GPC-method, yield the same increase as shown for $\bar{M}_v$ in Table I (PET-3: $\bar{M}_w = 50\,730$, $\bar{M}_n = 22\,450$, $\bar{M}_w:\bar{M}_n = 2.26$; PET-8:$\bar{M}_w = 73\,700$, $\bar{M}_n = 28\,100$, $\bar{M}_w:\bar{M}_n = 2.61$).

The light optical micrographs given in Fig. 2 illustrate that for crystallinities up to about 28% no spherulitic morphology develops during the thermal history (Fig. 2a valid for specimens PET-6 to 8). All the other samples possessed a microspherulitic structure as given in Fig. 2b.

3.2. Mechanical response

Considering the different crystallinity–molecular weight combinations, a variety in the shape of the load–displacement curves of the different PET specimens has to be expected. In fact, Fig. 3 shows five curves of different characteristics which can be correlated with special combinations of the two dominant microstructural parameters. In a first approximation it can be stated that in the case of a low degree of crystallinity and a moderately high molecular weight, the elongation to fracture is high but at the cost of a low resistance to plastic deformation (expressed by a low value of maximum stress). On the other hand, a high degree of crystallinity leads to a higher modulus as well as higher stresses before any kind of damage zone can develop at the tip of the initial notch and before further failure of the specimens occurs. A very extreme behaviour is measured with specimens of type PET-5 which behave in a completely brittle manner at very low stresses.

The following data were taken from the load–

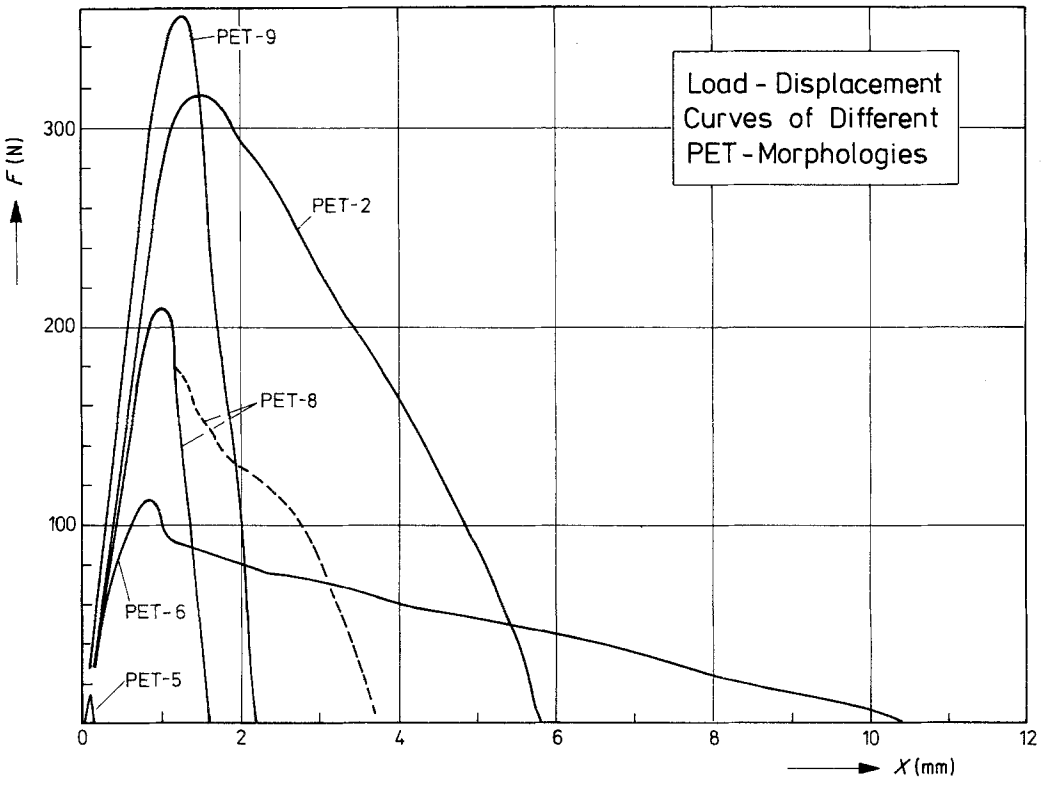

Figure 3 Load–displacement curves typical for different morphologies in the notched samples tested.

displacement curves: initial slope ($N\,m^{-1}$), maximum load (N), the work to achieve the maximum load (Nm), and the total work to fracture the specimens (Nm). In order to demonstrate relative changes and to relate to more fundamental parameters, these values were normalized by dividing by the same parameter from "standard" specimens. Chosen for the standard was material PET-6, that means the one with the lowest amount of crystallinity. Since the initial slope is directly proportional to the tensile modulus, the normalized slope, E^*, represents the ratio of moduli between a given specimen and the standard. In the same way, the normalized work to attain the load maximum, W^*_{max}, is the work of failure initiation ratio between the given specimen and the standard. Similar relationships hold for the work to failure, W^*_{tot}. The normalized maximum stress, σ^*_{max}, is loosely related to the ratio of the notch tensile strengths [28].

Fig. 4 shows the changes of normalized modulus, and ultimate stress as a function of the degree of crystallinity. In spite of broad differences in the molecular weight a linear increase in both material properties with the amount of crystallinity is observed. The only exception is found for material PET-5 with respect to its very low strength. The results are in agreement with investigation on the influence of crystallinity on modulus and strength of other thermoplastic polymers, and the explanation for these correlations are based on the higher molecular orientation with increasing degree of crystallinity which gives rise to a higher modulus. In addition, the higher intermolecular bonding in the crystalline regions as well as the effect of the crystals to act as local contact-points of high resistance against plastic deformation (as long as the molecular weight is high enough to provide strong bonding between these local knots) yield higher values of stresses necessary to cause plastic deformation.

The correlations with the degree of crystallinity are, however, no longer significant when considering the work to failure initiation and especially the total work to fracture (Fig. 5). In these cases, five characteristic regions of different deformational behaviour are found, especially if one considers the energy required for the final separation of the samples after failure initiation. At the same time, the energy values do not correspond in a

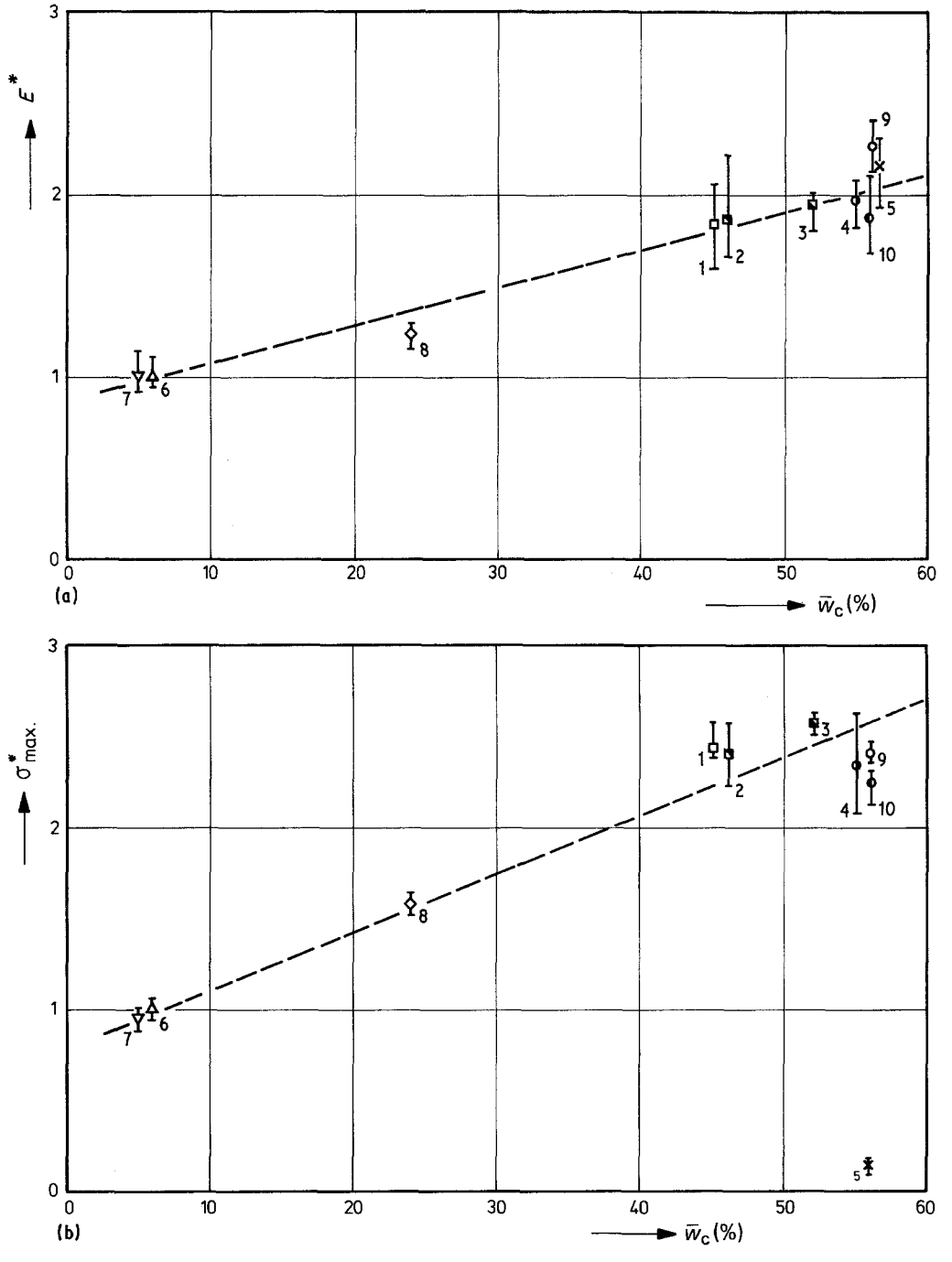

Figure 4 (a) Normalized elastic modulus, E^*, as a function of the averaged degree of crystallinity, $\bar{w}_c$. (b) Normalized maximum notch stress σ^*_{max} as a function of average degree of crystallinity, $\bar{w}_c$. The individual numbers at each of the scatter bars characterize the type of materials as given in Table I.

simple way with the molecular weight of the materials investigated. In other words, it is obviously the combination of molecular weight and degree and perfection of the crystalline arrays which determines whether the material exhibits a high energy to failure or not. Before discussing the optimum conditions of molecular weight and degree of crystallinity in more detail, it seems to be promising to elucidate first the possible modes of failure as a function of the different molecular weight–crystallinity combinations.

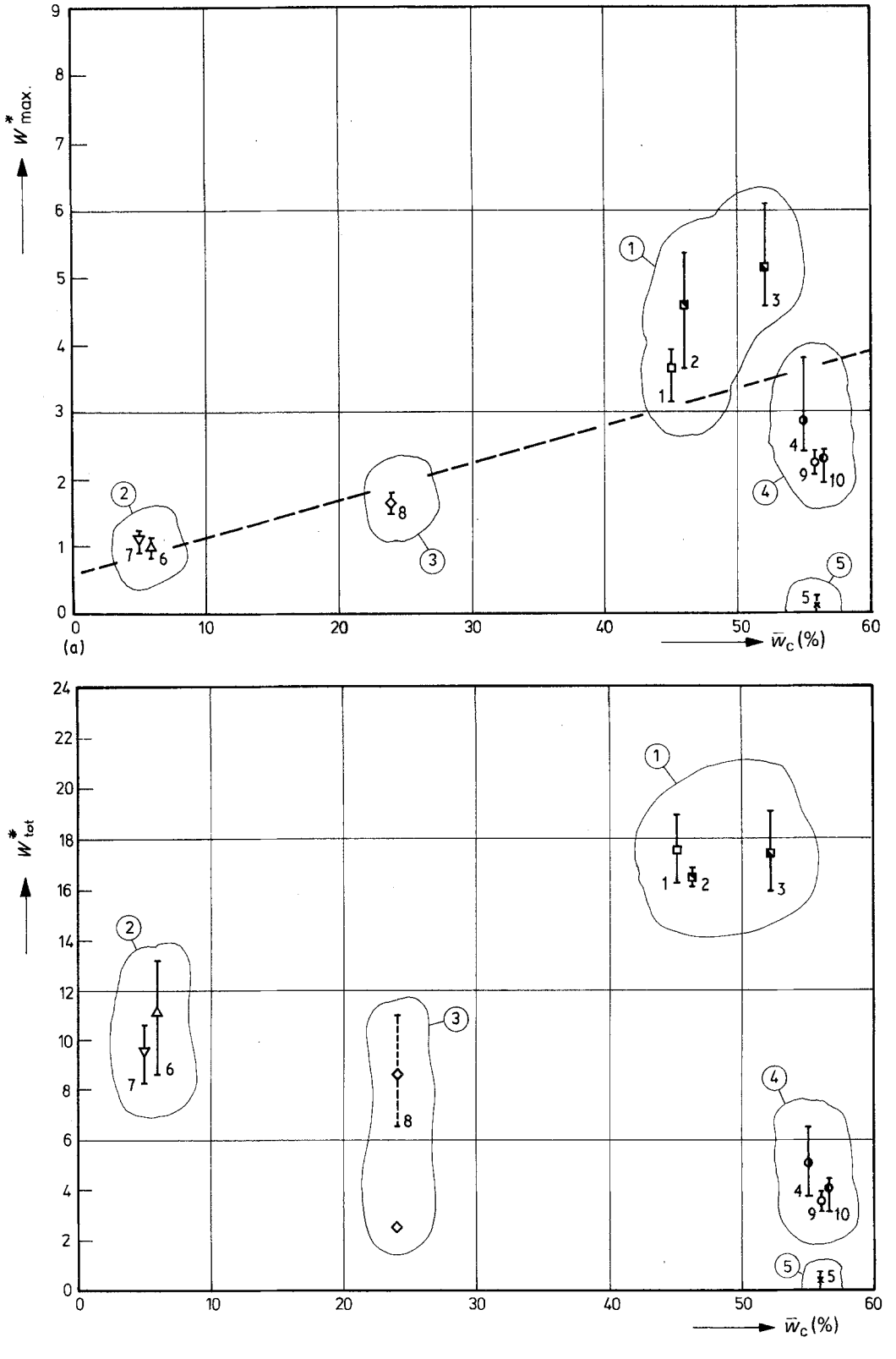

Figure 5 Work of failure initiation, W^*_{max} (a) and total work to fracture, W^*_{tot} (b) related to changes in degree of crystallinity. In both cases, the values were normalized to the work of failure initiation as measured for PET-6. The individual regions 1 to 5 summarize materials with a particular failure behaviour.

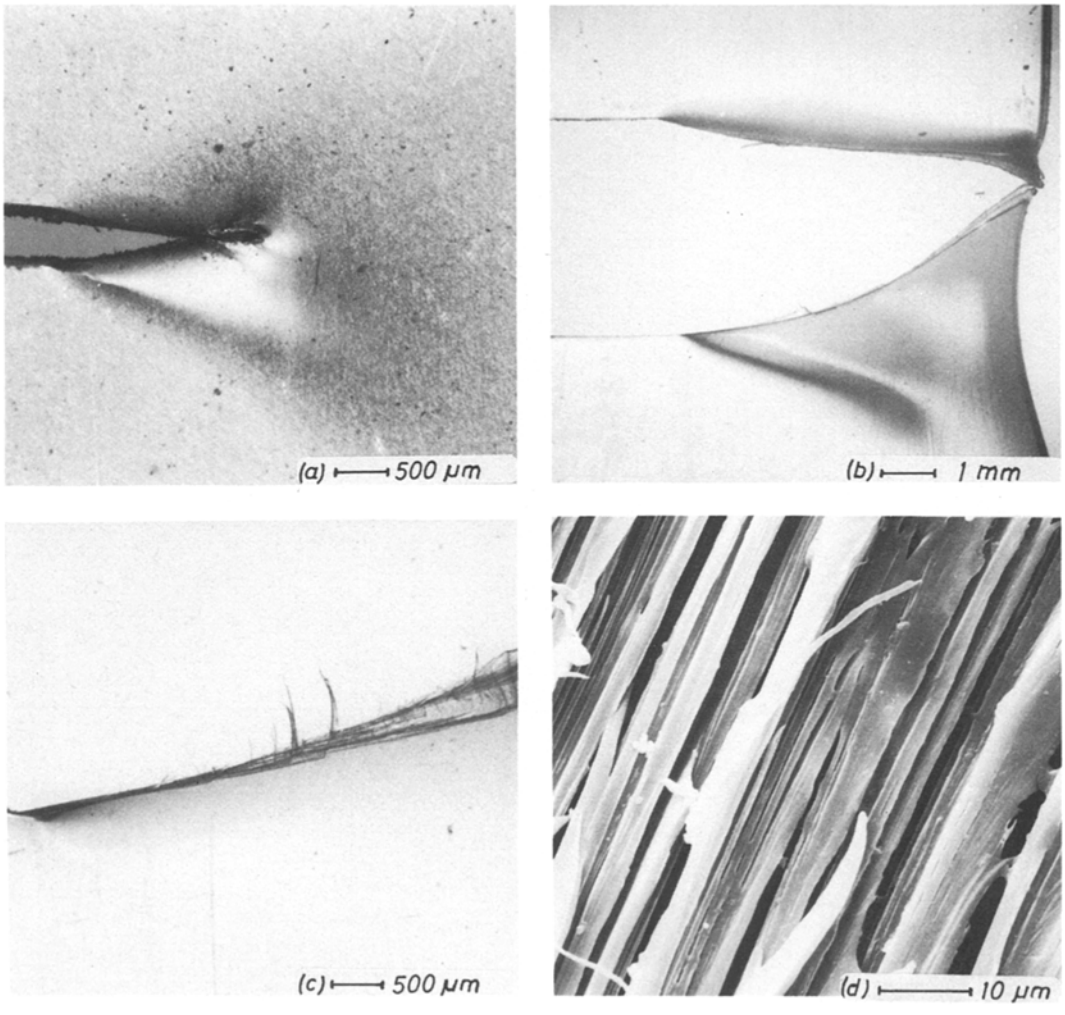

Figure 6 Characteristic failure events during breakdown of materials of Group 1: (a) Formation of a broad and wide plastic deformation zone in front of the initial notch (crack growth from left to right) and (b) material separation along one edge of the highly deformed region. (c) A higher magnification of the fracture edge profile, indicating, similar to the SEM-fracture surface micrograph (d), the microstructural transformation into a fibrillar structure before rupture of the material.

3.3. Analysis of failure mechanisms

3.3.1. Microscopic observations

As already indicated in the diagram of the total work to fracture as a function of crystallinity (Fig. 5) as well as in the different shape of the load–displacement curves (Fig. 3), there exist five material groups which differ in deformational behaviour. In fact, analysing microscopically the notched tensile test samples of the individual regions marked in Fig. 5 leads to five types of different failure characteristics. Group 1 combines materials PET-1 to 3 (moderately low molecular weight and moderately high degree of crystallinity). Fig. 6 shows that the propagation of the initial crack through the rest cross section of the sample is associated with a high degree of plastic deformation of the material in front of the crack tip. This, in turn, has two positive effects with respect to the fracture behaviour of the material. On the one hand, high stresses are necessary to transform the crystalline spherulitic morphology into a highly oriented structure. On the other hand, as the transformation occurs in a very large volume, a high amount of energy for such a morphological transformation is required. That means, high stresses as well as high local strains must be exceeded before such a deformed, fibrillar microstructure can be separated to enable crack propagation.

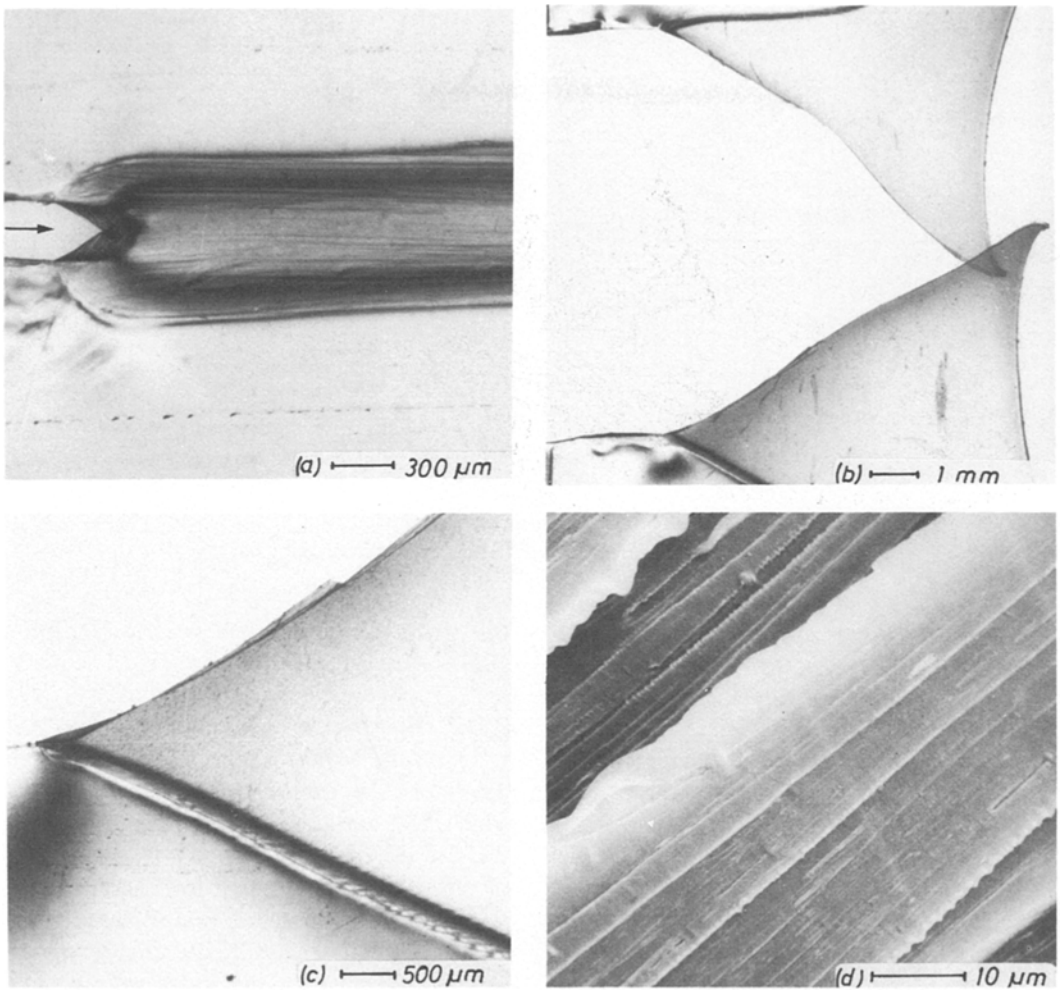

Figure 7 Analogous micrographs (as discussed in Fig. 6) for materials of Group 2: (a) initiation of a narrow highly necked region in front of the initial notch (arrow), (b) parts of a ruptured specimen, (c) higher magnification of the damaged zone and the fracture profile, and (d) fracture surface appearance.

The deformation mechanisms found in Group 2 are similar in appearance to those found in Group 1 although the materials which belong to this group have a quite different molecular weight–crystallinity relationship (materials PET-6 and 7). The difference with respect to Group 1 is that the transformation from the non-deformed, nearly non-crystalline microstructure into a highly deformed region in front of the crack tip only occurs in a narrow neck of material in the notch cross-section. The result is a relatively low stress as well as energy before failure initiation (Fig. 7). Subsequent crack progress is associated with further plastic deformation of the pre-deformed notch cross-section. Owing to the moderately high molecular weight of this material group, a high amount of strain is required before a film like material separation can take place.

An enhancement of degree of crystallinity at this level of molecular weight leads to a mixture of different failure modes (Group 3; different from specimen to specimen) which indicates that at high molecular weight levels the degree of crystallinity can cause a transition from highly ductile to semi-brittle fracture behaviour (Fig. 8). In fact, increasing the degree of crystallinity furthermore (associated with a simultaneous increase in the molecular weight) leads to the specimens of Group 4 which all have failed after initial craze formation in a semi-brittle manner. Fig. 9 illustrates the individual steps during breakdown of this type of material (PET-4, 9 and 10). After the

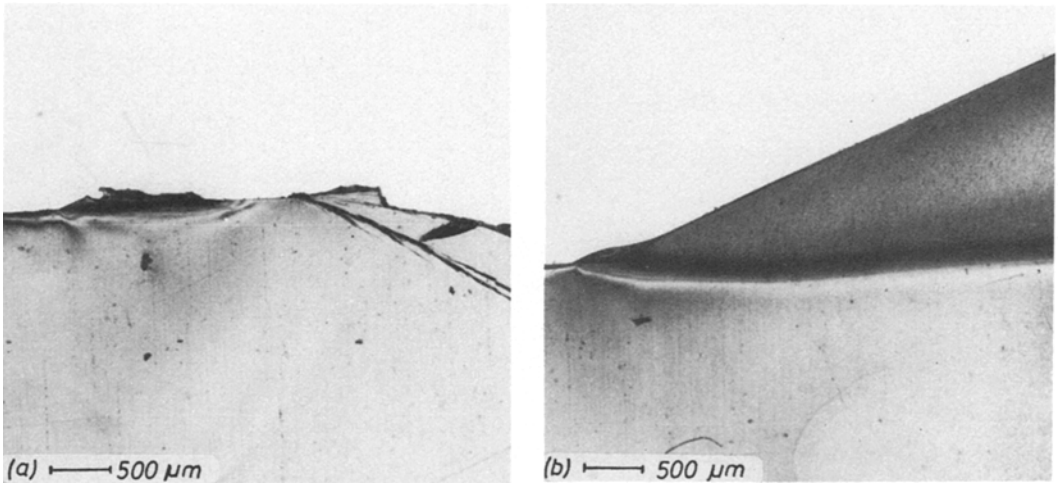

Figure 8 Comparison of the different possible failure modes of materials in Group 3: (a) initially ductile with transition to a brittle fracture, (b) completely ductile mode of failure, similar to that described in Fig. 7.

formation of a small straight bundle of individual crazes in front of the notch (Fig. 9a), material separation occurs first in a ductile way due to a coalescence of densely packed crazes in a rather small material volume. As this process incorporates the transformation of highly crystalline material into a fibrillar structure, relatively high stresses are necessary. However, once a crack has started, crack acceleration into one of the individual crazes will soon take place. In this way, sharpening of the crack tip occurs which at the same time leads to an enhancement of the stress intensity in front of this tip. This is associated with further speeding up of the crack until reaching the tip of the craze in front of it. At that moment, crack instability occurs which is clearly marked on the fracture surface by a sharp line (Fig. 9d). The patchwork pattern on the left-hand side of this line is a typical indicator for the separation of craze matter at the upper or lower craze edge due to accelerated propagation of a crack through a craze. From this point, the energy required for brittle fracture of the rest of the specimen is comparably low to the conditions described for Groups 1 and 2 so that the total work to fracture does not differ very much from the work to failure initiation.

Finally, Fig. 10 shows the fracture profile of material Group 5 (PET-5). The low magnification micrographs document an absolutely brittle behaviour. However, at very high magnifications, even in the brittle case, local tips of deformed material, which look like separated fibrils of very low fibril density, are found in various regions of the brittle fracture surface given in Fig. 10b (Fig. 10c).

3.2.2. Macroscopic classification and failure map

The molecular weight–crystallinity combinations which lead to the characteristic failure modes of the five different groups can be classified macroscopically in the following way (Fig. 11):

Group 1: moderately low molecular weight and moderately high degree of crystallinity;

Group 2: medium molecular weight and very low degree of crystallinity;

Group 3: medium molecular weight and moderately low degree of crystallinity;

Group 4: high degree of crystallinity and moderately high to high molecular weight;

Group 5: high degree of crystallinity and low molecular weight.

In order to understand, for example, the effect of molecular weight for a given degree in crystallinity or the effect of crystallinity for a material with a given molecular weight, one can perform a stepwise consideration from one material group to the other in a way that one tries to keep one of the two main material parameters nearly constant. Transition I from material Group 1 to material Group 2 gives an idea what changes in failure behaviour as well as in particular mechanical properties have to be expected when a slight increase in the molecular weight is associated with a simultaneously high reduction in the degree of crystallinity. The latter causes a highly reduced stress

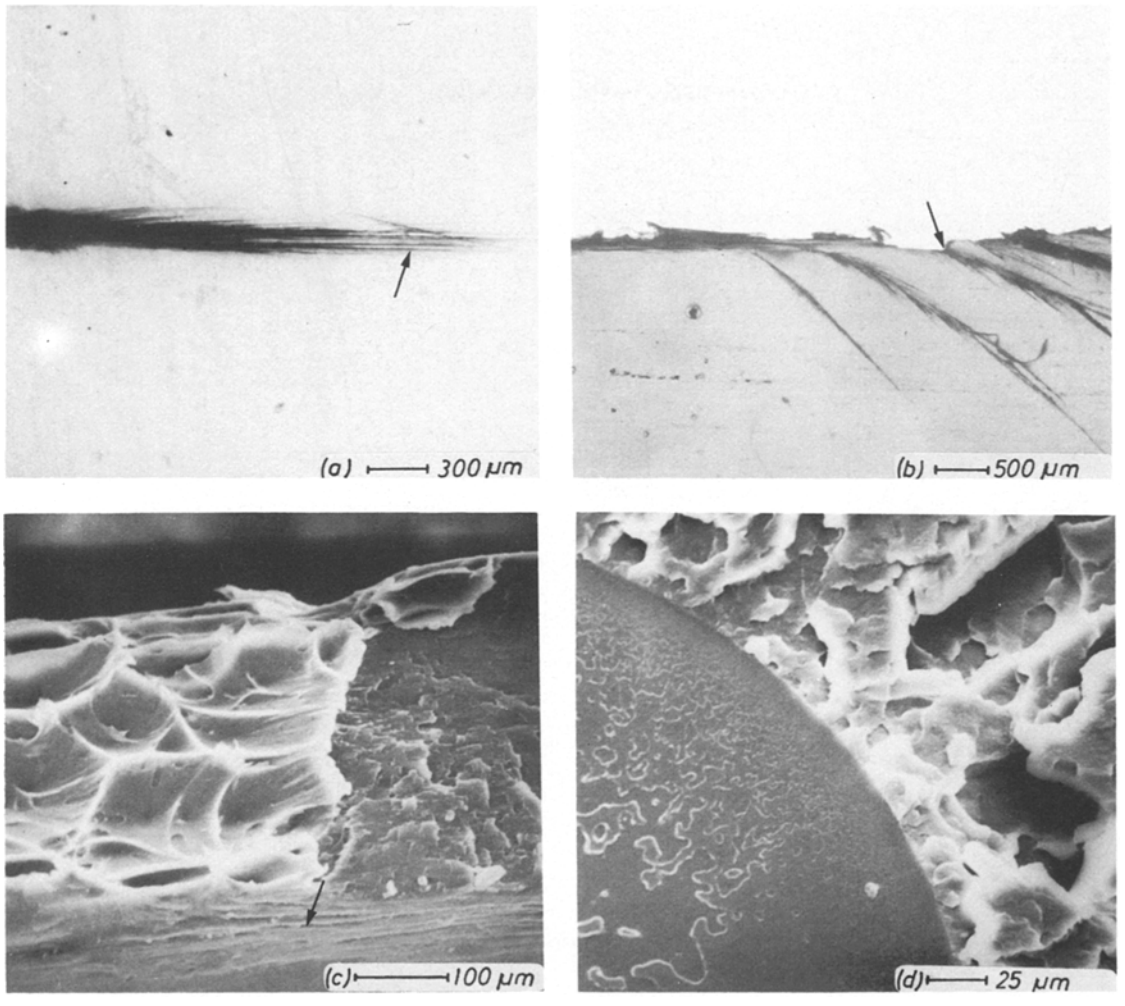

Figure 9 (a) Formation of a dense craze bundle (arrow) in front of a crack in material PET-8 (Group 4) and (b) semi-ductile, subcritical crack growth with subsequent transition to a brittle fracture mode (combined with local crack bifurcation (arrow)). (c) The fracture surface appearance in the initial, semi-ductile zone which develops in the region of the dense craze bundle (arrow); (d) the transition from craze-controlled cracking to the final part of brittle crack instability.

level for the initiation of a damage zone, whereas the slightly higher molecular weight provides a greater elongation to break. Transition II indicates the tendencies which arise when in a material with medium molecular weight level the degree of crystallinity is clearly enhanced. Under these circumstances the stress necessary to initiate damage in front of a notch is higher, but at the cost of the energy to total failure of the material. Increasing the degree of crystallinity still further (transition III from material Group 3 to Group 4) leads to failure modes typical for semi-brittle materials.

At relatively high stresses, the initiation of a damage zone is localized in the form of a dense bundle of individual crazes from which further crack development, first in a ductile but finally in a brittle mode of propagation, takes place. In this region no remarkable influence of a further increase in molecular weight is detectable, which is probably due to the fact that the higher degree of crystallinity in these materials is accompanied by an additionally higher perfection of the crystalline regions. This fact must be assumed to be of negative influence on the fracture behaviour of a thermoplastic material and superimposes those positive effects which usually arise from a higher molecular weight.

Transition IV may give an impression of the

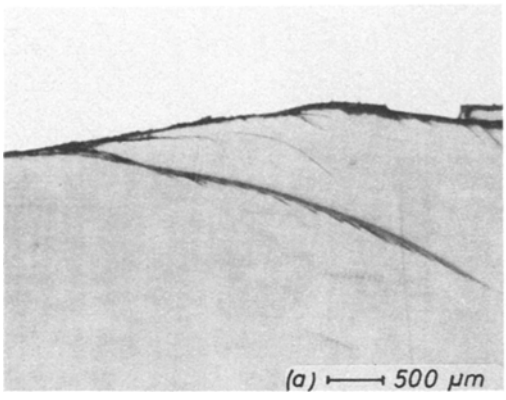

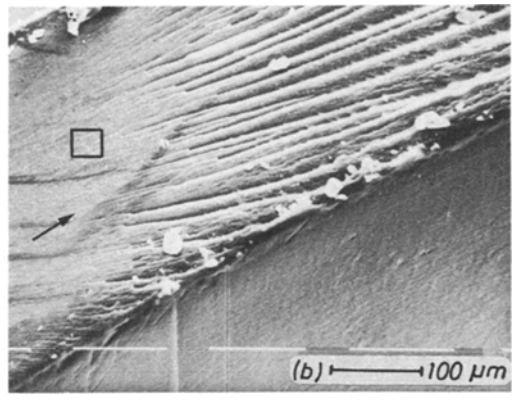

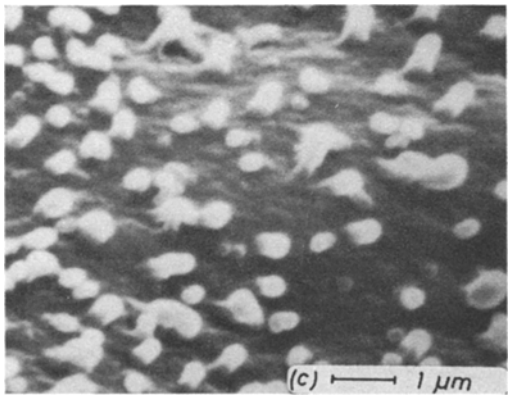

Figure 10 Absolutely brittle fracture profile with low degree of bifurcation (a) in material PET-5 (Group 5); (b) represents the appearance of the corresponding fracture surface (arrow = crack direction). At very high magnification, local tips of plastically deformed polymer are detectable (c).

deleterious results which can occur when in a material with a very high amount of crystallinity the molecular weight is highly reduced (material Group 4 to material Group 5). In addition to the high perfection of crystal arrays which itself leads to a localization of the deformation in the form of individual crazes (which are in the case of a high molecular weight still very numerous, which form only after a relatively high stress level is reached, and which provide, at least in the beginning of failure, a certain degree of ductility) the density and strength of the intercrystalline strands is highly reduced. The consequence of both effects results in a very brittle, low strength material in which crack propagation immediately occurs as soon as one minor defect in front of the initial notch has been created. No chance for a stabilization of localized defects as in the case of the formation of a dense craze bundle exists.

The results of the failure mode analysis can be summarized in a failure map in which the area of the molecular weight as a function of degree of

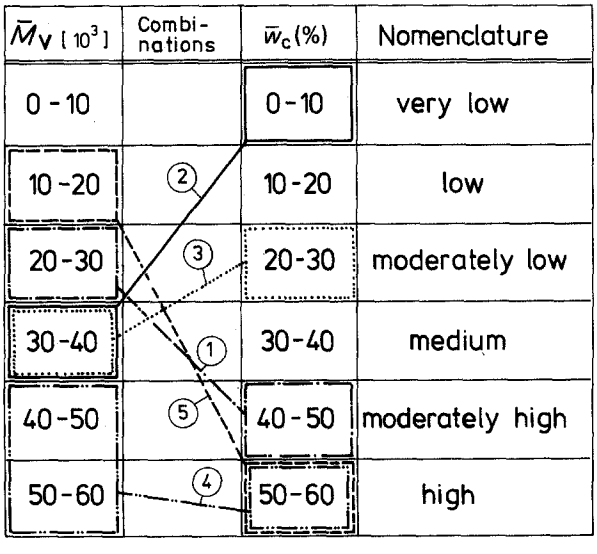

Figure 11 Classification of the individual materials into Groups 1 to 5 characterized by a particular combination of molecular weight and degree of crystallinity.

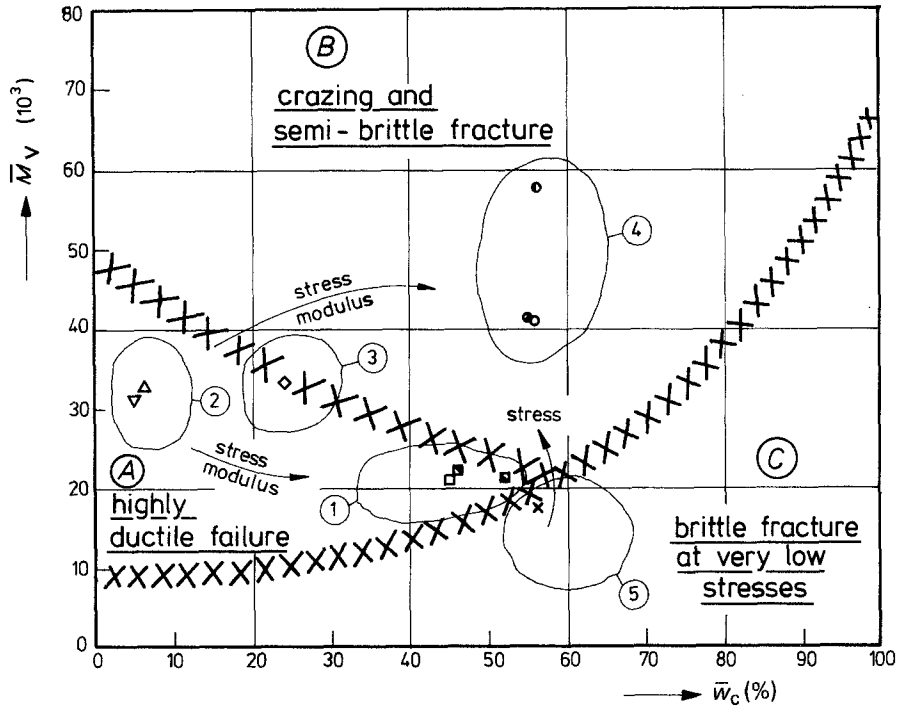

Figure 12 Map classifying domains of different failure mode (A, B, C) as a function of molecular weight–crystallinity combination in various morphologies of PET. In addition, arrows indicate increasing tendencies of ultimate stress and elastic modulus.

crystallinity is divided into different regions of similar failure behaviour as shown in Fig. 12. Three characteristic failure domains can be distinguished. Materials in domain A fail in a highly ductile manner, although it should be mentioned that the stresses to initiate this kind of failure can be very different. The optimum condition with respect to high ultimate stresses as well as high total energy to failure is found for the case of moderately low molecular weight and moderately high degree of crystallinity. On the other hand, in this region of the failure map, transitions to yet higher degree of crystallinity or to higher or lower molecular weights can easily be associated with a tremendous change in the failure behaviour. For instance, an increase in molecular weight leads to domain B for which, at high ultimate stresses, fracture occurs after crazing, finally in a semi-brittle mode. Changes in the other direction are even more critical. In this case one approaches domain C in which the material tends to fail in a completely brittle fracture mode already at very low stresses.

4. Concluding remarks

The results of fracture studies of notched polyethylene terephthalate ribbons as a function of different kinds of thermal treatment by which variations in both the molecular weight as well as the degree of crystallinity were derived, have shown that depending on the molecular weight–crystallinity relationship fracture can occur at high or low stresses and/or after the absorption of a high or a low amount of energy to failure. Usually, a maximum in both properties, i.e. in the resistance of a material against plastic deformation (maximum yield stress) and in the resistance against crack propagation and fracture (total energy to failure) is required. As all of these requirements usually cannot be fulfilled simultaneously, material development must centre at an optimum of both. This is probably approached when the product of both properties is at its maximum. Such a product was recently defined by Hornbogen [29] as a more relevant term for the real "strength" of a material. Following his suggestions, it becomes clearer that the best molecular weight–crystallinity combinations of the material studied in this investigation are those of Group 1 having a moderately low molecular weight and a moderately high degree of crystallinity. Fig. 13 illustrates, in a double logarithmic scale, how the individual

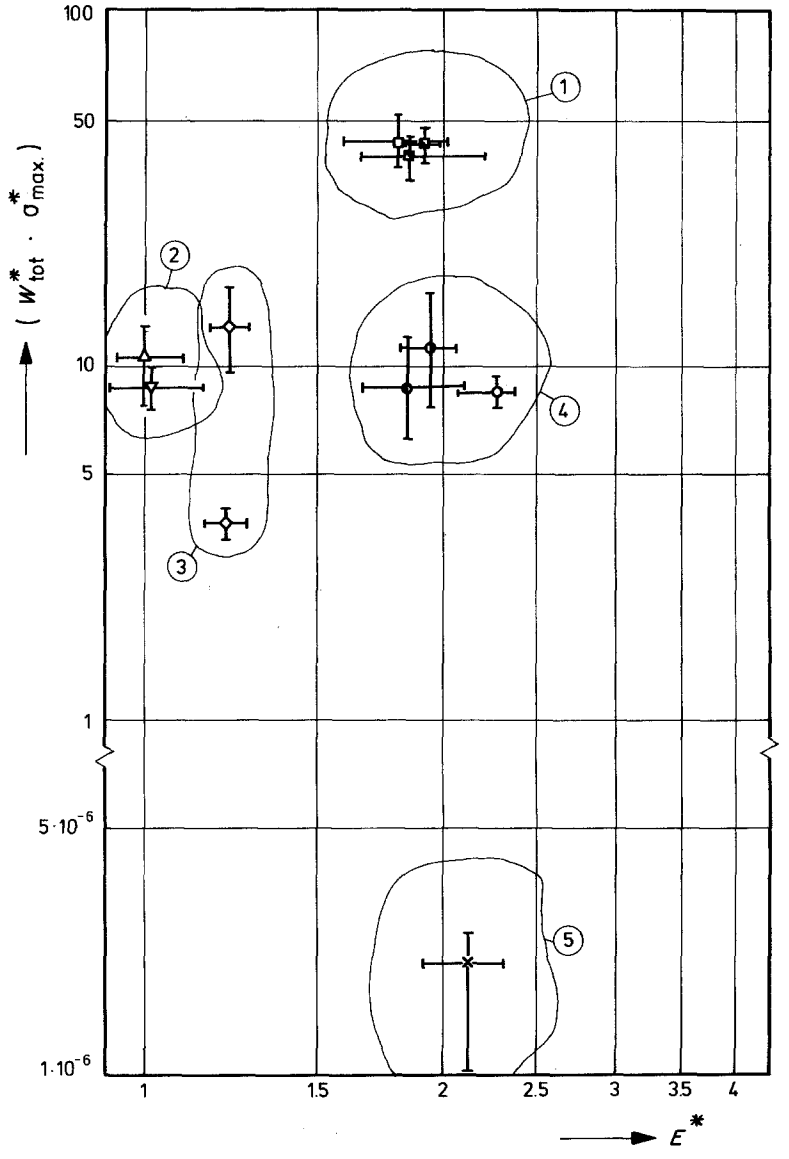

Figure 13 Relative amounts of optimum "strength", defined as the product of total fracture energy and ultimate stress, plotted against the elastic modulus of material Groups 1 to 5.

material groups differ with respect to the newly defined strength term when plotted against the elastic modulus as the other important property for construction materials.

Finally, if one takes the average value of "strength" found in each of the five different material groups one can come to a three-dimensional presentation. Fig. 14 illustrates plastically how variations in molecular weight and/or degree of crystallinity yield changes in both failure mode as well as the value of strength defined as a product of ultimate yield stress and total work to failure. It should be mentioned, however, that the location of the boundaries indicating the transition from one failure behaviour to the other associated with drastic changes in the strength of the materials has been derived only from discrete points of molecular weight/crystallinity combination. Therefore, they are drawn at present relatively vaguely which is in the present case indicated by the broad crossed lines. More measurements for a wider variety of molecular weight–crystallinity pairs are necessary in order to find the actual limitations exactly. Nevertheless it can be concluded from the studies

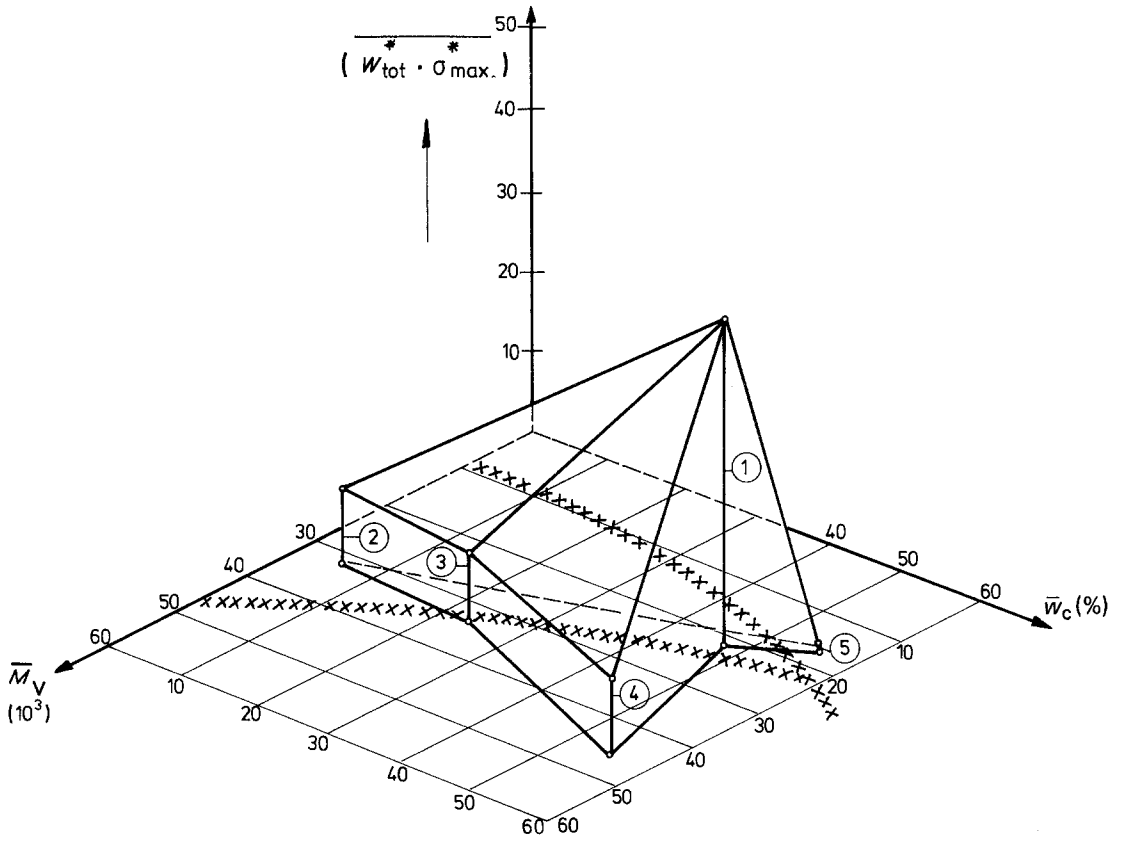

Figure 14 Average values of "strength" as a function of both molecular weight and degree of crystallinity in different PET-materials.

presented here that the fracture behaviour of semi-crystalline thermoplastic materials is clearly a function of a combination of different molecular and morphological parameters and that when changing one parameter systematically and holding the other constant, not always a systematic change in one particular mechanical property of the material can be expected.

Acknowledgements

The study was performed by both authors during a research stay in 1983 at the Department of Chemical Engineering and the Center for Composite Materials, University of Delaware, Newark, Delaware 19716, USA. Thanks are due to Professor R. B. Pipes and Professor J. M. Schultz, with whose facilities the experiments were carried out.

References

1. J. M. SCHULTZ, "Polymer Materials Science" (Prentice Hall, Englewood Cliffs, New Jersey, 1974).
2. J. H. MAGILL, in "Treatise on Materials Science and Technology", Vol. 10, Part A, edited by J. M. Schultz (Academic Press, New York, 1977).
3. R. P. KAMBOUR and R. E. ROBERTSON, in "Polymer Science", Vol 1, edited by A. D. Jenkins (North Holland, Amsterdam, 1972).
4. E. H. ANDREWS, *ibid.*
5. H. H. KAUSCH, "Polymer Fracture" (Springer Verlag, Berlin, 1978).
6. K. FRIEDRICH, in "Advances in Polymer Science 52/53", (Springer Verlag, Berlin, 1983).
7. A. RAMIREZ, J. A. MANSON and R. W. HERTZBERG, *Polym. Eng. Sci.* **15** (1982) 975.
8. R. W. HERTZBERG and J. A. MANSON, "Fatigue of Engineering Plastics" (Academic Press, New York, 1980).
9. P. B. BOWDEN and R. J. YOUNG, *J. Mater. Sci.* 9 (1974) 2034.
10. P. H. GEIL, in "Fracture Processes in Polymer Solids", edited by B. Rosen (Interscience, New York, 1964).
11. A. J. KINLOCH and R. J. YOUNG, "Fracture Behaviour of Polymers" (Applied Science, London, 1983).
12. J. A. MANSON and R. W. HERTZBERG, *Crit. Rev. Macromol. Sci.* **1** (1973) 433.
13. J. L. WAY, J. R. ATKINSON and J. NUTTING, *J. Mater. Sci.* 9 (1974) 293.
14. J. H. REINSHAGEN and R. W. DUNLAP, *J. Appl. Polymer Sci.* **20** (1976) 9.
15. H. D. KEITH, F. J. PADDEN Jr and R. G. VADIMSKY, *J. Appl. Phys.* **42** (1971) 4585.
16. K. FRIEDRICH, *Prog. Colloid Polymer Sci.* **64**

(1978) 103.
17. *Idem, ibid.* **66** (1979) 299.
18. H. R. ALLCOCK and F. W. LAMPE, "Contemporary Polymer Chemistry" (Prentice Hall, Englewood Cliffs, New Jersey, 1981).
19. S. FAKIROV, *Colloid Polymer Sci.* **256** (1978) 115.
20. S. FAKIROV and D. STAHL, *Die. Angew. Makromol. Chemie* **102** (1982) 117.
21. E. W. FISCHER and S. FAKIROV, *J. Mater. Sci.* **11** (1976) 1041.
22. W. GRIEHL, *Faserforsch. u. Textiltechn.* **5** (1954) 423.
23. B. WUNDERLICH, "Macromolecular Physics", Vol. 1 (Academic Press, New York, 1973).
24. C. W. SMITH and M. DOLE, *J. Polym. Sci.* **20** (1956) 37.
25. J. BRANDRUP and E. H. IMMERGUT, "Polymer Handbook" (Interscience, New York, 1966).
26. S. FAKIROV, E. W. FISCHER and G. F. SCHMIDT, *Macromol. Chem.* **176** (1975) 2459.
27. S. FAKIROV, E. W. FISCHER, R. HOLTMANN and G. F. SCHMIDT, *Polymer* **18** (1977) 1121.
28. J. M. SCHULTZ and K. FRIEDRICH, *J. Mater. Sci.* **19** (1984) 2246.
29. E. HORNBOGEN, *Z. Metallkde.* **68** (1977) 455.

Received 20 August
and accepted 13 September 1984